

Limits on gravitational wave emission from selected pulsars using LIGO data

B. Abbott,¹² R. Abbott,¹⁵ R. Adhikari,¹³ A. A. Gevez,^{20,27} B. Allen,³⁹ R. Ammend,³⁴ S. B. Anderson,¹² W. G. Anderson,²⁹ M. A. Araya,¹² H. Armandula,¹² M. Ashley,²⁸ F. A. Siri,^{12,a} P. Aufmuth,³¹ C. Aubert,¹ S. Babak,⁷ R. Balasubramanian,⁷ S. Ballmer,¹³ B. C. Barish,¹² C. Barker,¹⁴ D. Barker,¹⁴ M. Barnes,^{12,b} B. Barr,³⁵ M. A. Barton,¹² K. Bayar,¹³ R. Beausoleil,^{26,c} K. Belczynski,²³ R. Bennett,^{35,d} S. J. Benko,^{1,e} J. Betzwieser,¹³ B. Bhawal,¹² I. A. Bilenko,²⁰ G. Billingsley,¹² E. Black,¹² K. Blackburn,¹² L. Blackburn,¹³ B. Blaßland,¹⁴ B. Bochner,^{13,f} L. Bogue,¹² R. Bork,¹² S. Bose,⁴⁰ P. R. Brady,³⁹ V. B. Braginsky,²⁰ J. E. Brau,³⁷ D. A. Brown,³⁹ A. Bulingting,²⁶ A. Bunkowski,^{2,31} A. Buonanno,^{6,g} R. Burgess,¹³ D. Busby,¹² W. E. Butler,³⁸ R. L. Byer,²⁶ L. Cadonati,¹³ G. Cagnoli,³⁵ J. B. Camp,²¹ C. A. Cantley,³⁵ L. Cardenas,¹² K. Carter,¹⁵ M. M. Casey,³⁵ J. Castiglione,³⁴ A. Chandler,¹² J. Chapsky,^{12,b} P. Charlton,¹² S. Chatterji,¹³ S. Chelkowski,^{2,31} Y. Chen,⁶ V. Chickamane,^{16,h} D. Chin,³⁶ N. Christensen,⁸ D. Churches,⁷ T. Cokelaer,⁷ C. Colacino,³³ R. Coldwell,³⁴ M. Coles,^{15,i} D. Cook,¹⁴ T. Corbitt,¹³ D. Coyne,¹² J. D. E. Creighton,³⁹ T. D. E. Creighton,¹² D. R. M. Crooks,³⁵ P. C. Satorday,¹³ B. J. Cusack,³ C. Cutler,¹ E. D'Ambrasio,¹² K. Danzmann,^{31,2} E. Daw,^{16,j} D. DeBra,²⁶ T. Deller,^{34,k} V. Dergachev,³⁶ R. DeSalvo,¹² S. Dhurandhar,¹¹ A. Di Credico,²⁷ M. Diaz,²⁹ H. Ding,¹² R. W. Drever,⁴ R. J. Dupuis,³⁵ J. A. Edlund,^{12,b} P. Ehrens,¹² E. J. Elliott,³⁵ T. Etzel,¹² M. Evans,¹² T. Evans,¹⁵ S. Fairhurst,³⁹ C. Fallnich,³¹ D. Farmham,¹² M. M. Fejer,²⁶ T. Finley,²⁵ M. Fine,¹² L. S. Finn,²⁸ K. Y. Franzen,³⁴ A. Freise,^{2,1} R. Frey,³⁷ P. Fritschel,¹³ V. V. Frolov,¹⁵ M. Fyffe,¹⁵ K. S. Ganezer,⁵ J. Garafoli,¹⁴ J. A. Giaime,¹⁶ A. Gillepie,^{12,m} K. Goda,¹³ G. Gonzalez,¹⁶ S. Goerner,³¹ P. Grandclement,^{23,n} A. Grant,³⁵ C. Gray,¹⁴ A. M. G. Retarsson,¹⁵ D. Grinmatt,¹² H. Grote,² S. Grunewald,¹ M. Guenther,¹⁴ E. Gustafson,^{26,o} R. Gustafson,³⁶ W. O. Hamilton,¹⁶ M. Hammond,¹⁵ J. Hanson,¹⁵ C. Hardham,²⁶ J. Hamm,¹⁹ G. Harry,¹³ A. Hartmanian,¹² J. Heefner,¹² Y. Heftz,¹³ G. Heinzel,² I. S. Heng,³¹ M. Hennessy,²⁶ N. Hepler,²⁸ A. Heptonstall,³⁵ M. Heurs,³¹ M. Hewitson,² S. Hild,² N. Hindman,¹⁴ P. Hoang,¹² J. Hough,³⁵ M. Hrynevych,^{12,p} W. Hua,²⁶ M. Ito,³⁷ Y. Itoh,¹ A. Ivanov,¹² O. Jennrich,^{35,q} B. Johnson,¹⁴ W. W. Johnson,¹⁶ W. R. Johnston,²⁹ D. I. Jones,²⁸ L. Jones,¹² D. Jungwirth,^{12,r} V. Kalogera,²³ E. Katsavounidis,¹³ K. Kawabe,¹⁴ S. Kawamura,²² W. Kells,¹² J. Kem,^{15,s} A. Khan,¹⁵ S. Killbourn,³⁵ C. J. Killow,³⁵ C. Kim,²³ C. King,¹² P. King,¹² S. Klimenko,³⁴ S. Koranda,³⁹ K. Kotter,³¹ J. Kovalik,^{15,b} D. Kozak,¹² B. Krishnan,¹ M. Landry,¹⁴ J. Langdale,¹⁵ B. Lantz,²⁶ R. Lawrence,¹³ A. Lazzarini,¹² M. Lei,¹² I. Leonor,³⁷ K. Lipprecht,¹² A. Libson,⁸ P. Lindquist,¹² S. Liu,¹² J. Logan,^{12,t} M. Lormand,¹⁵ M. Lubinski,¹⁴ H. Luck,^{31,2} T. T. Lyons,^{12,t} B. M. Achenschalk,¹ M. M. MacInnis,¹³ M. Mageswaran,¹² K. M. Ailand,¹² W. M. Ajid,^{12,b} M. M. Alec,^{2,31} F. M. Ann,¹² A. M. Arin,^{13,u} S. M. Arka,¹² E. M. Aros,¹² J. Mason,^{12,v} K. M. Mason,¹³ O. M. Athemy,¹⁴ L. M. Atone,¹⁴ N. M. Avalvala,¹³ R. M. McCarthy,¹⁴ D. E. Mc Cullard,³ M. M. Chugh,¹⁸ J. W. C. M. Cabb,²⁸ G. M. Endell,¹⁴ R. A. M. Eroer,³³ S. M. Eshkov,¹² E. M. Essaritaki,³⁹ C. M. Essenger,³³ V. P. M. Itrofanov,²⁰ G. M. Itselman,³⁴ R. M. Ittlemann,¹³ O. M. Iyakawa,¹² S. M. Iyoki,^{12,w} S. M. Chantz,²⁹ G. M. Oreno,¹⁴ K. M. Ossavi,² G. M. Ueller,³⁴ S. Mukherjee,²⁹ P. Murray,³⁵ J. Myers,¹⁴ S. Nagano,² T. Nash,¹² R. Nayak,¹¹ G. Newton,³⁵ F. Nocera,¹² J. S. Noel,⁴⁰ P. Nutzman,²³ T. Olson,²⁴ B. O'Reilly,¹⁵ D. J. Ottaway,¹³ A. Ottewill,^{39,x} D. Ouimette,^{12,r} H. Overmier,¹⁵ B. J. Owen,²⁸ Y. Pan,⁶ M. A. Papa,¹ V. Parameshwaraiah,¹⁴ C. Parameswaran,¹⁵ M. Pedraza,¹² S. Penn,¹⁰ M. P. Pitkin,³⁵ M. P. Lissi,³⁵ R. P. Rix,¹ V. Q. Uetschke,³⁴ F. R. Raab,¹⁴ H. Radkins,¹⁴ R. Rahkola,³⁷ M. Rakhamanov,³⁴ S. R. Rao,¹² K. Rawlins,¹³ S. Ray-Majumder,³⁹ V. Re,³³ D. Redding,^{12,b} M. W. Regehr,^{12,b} T. Regenbauer,⁷ S. Reid,³⁵ K. T. Reilly,¹² K. Reithmaier,¹² D. H. Reitze,³⁴ S. Richman,^{13,y} R. Riesen,¹⁵ K. Riles,³⁶ B. Rivera,¹⁴ A. Rizzi,^{15,z} D. I. Robertson,³⁵ N. A. Robertson,^{26,35} L. Robison,¹² S. Roddy,¹⁵ J. Rollins,¹³ J. D. Romano,⁷ J. Romie,¹² H. Rong,^{34,m} D. Rose,¹² E. Rottho,²⁸ S. Rowan,³⁵ A. Rüdiger,² P. Russell,¹² K. Ryan,¹⁴ I. Salzman,¹² V. Sandberg,¹⁴ G. H. Sanders,^{12,aa} V. Sannibale,¹² B. Sathyaprakash,⁷ P. R. Saulson,²⁷ R. Savage,¹⁴ A. Sazonov,³⁴ R. Schilling,² K. Schlaufman,²⁸ V. Schmidt,^{12,bb} R. Schnabel,¹⁹ R. Schold,³⁷ B. F. Schutz,^{1,7} P. Schwinberg,¹⁴ S. M. Scott,³ S. E. Seader,⁴⁰ A. C. Searle,³ B. Sears,¹² S. Seel,¹² F. Seifert,¹⁹ A. S. Sengupta,¹¹ C. A. Shapiro,^{28,cc} P. Shawhan,¹² D. H. Shoemaker,¹³ Q. Z. Shu,^{34,dd} A. Sibley,¹⁵ X. Siemens,³⁹ L. Sievers,^{12,b} D. Sigg,¹⁴ A. M. Sintes,^{1,32} J. R. Smith,² M. Smith,¹³ M. R. Smith,¹² P. H. Sneddon,³⁵ R. Spero,^{12,b} G. Stapfer,¹⁵ D. Steussy,⁸ K. A. Strain,³⁵ D. Strom,³⁷ A. Stuver,²⁸ T. Summerscales,²⁸ M. C. Sumner,¹² P. J. Sutton,¹² J. Sylvestre,^{12,ee} A. Takamori,¹² D. B. Tanner,³⁴ H. Tariq,¹² I. Taylor,⁷ R. Taylor,¹² R. Taylor,³⁵ K. A. Thome,²⁸ K. S. Thome,⁶ M. Tibbets,²⁸ S. Tilav,¹² M. Tinto,^{4,b} K. V. Tokmakov,²⁰ C. Torres,²⁹ C. Torrie,¹² G. Traylor,¹⁵ W. Tyler,¹² D. Uglolini,³⁰ C. Ungarelli,³³ M. Vallisneri,^{6,gg} M. van Putten,¹³ S. Vass,¹² A. Vecchio,³³ J. Veitch,³⁵ C. Vorick,¹⁴ S. P. Vyachanin,²⁰ L. W. Wallace,¹² H. W. alther,¹⁹ H. W. ard,³⁵ B. W. are,^{12,b} K. W. atts,¹⁵ D. W. ebber,¹² A. W. eidner,¹⁹ U. W. eiland,³¹ A. W. einstein,¹² R. W. eiss,¹³ H. W. elling,³¹ L. W. en,¹² S. W. en,¹⁶ J. T. W. helan,¹⁸ S. E. W. hitcom,¹² B. F. W. hiting,³⁴ S. W. iley,⁵ C. W. ilkinson,¹⁴ P. A. W. illem,¹² P. R. W. illiam,^{s,1,hh} R. W. illiam,^{s,4} B. W. ilke,³¹ A. W. ilson,¹² B. J. W. injum,^{28,e} W. W. inkler,² S. W. ise,³⁴ A. G. W. isem,^{an,39} G. W. oan,³⁵ R. W. orden,¹⁴ W. W. u,³⁴ I. Yakushin,¹⁵ H. Yamamoto,¹² S. Yoshida,²⁵

K. D. Zaleski,²⁸ M. Zanolin,¹³ I. Zawischa,^{31,ii} L. Zhang,¹² R. Zhu,¹ N. Zotov,¹⁷ M. Zucker,¹⁵ and J. Zweizig¹²
(The LIGO Scientific Collaboration, <http://www.ligo.org>)

M. Krammer⁴¹ and A. G. Lyne⁴¹

¹Albert-Einstein-Institut, Max-Planck-Institut für Gravitationsphysik, D-14476 Golm, Germany
²Albert-Einstein-Institut, Max-Planck-Institut für Gravitationsphysik, D-30167 Hannover, Germany

³Australian National University, Canberra, 0200, Australia

⁴California Institute of Technology, Pasadena, CA 91125, USA

⁵California State University Dominguez Hills, Carson, CA 90747, USA

⁶Caltech-CaRT, Pasadena, CA 91125, USA

⁷Cardiff University, Cardiff, CF2 3YB, United Kingdom

⁸Carleton College, Northfield, MN 55057, USA

⁹Fermi National Accelerator Laboratory, Batavia, IL 60510, USA

¹⁰Hobart and William Smith Colleges, Geneva, NY 14456, USA

¹¹Inter-University Centre for Astronomy and Astrophysics, Pune - 411007, India

¹²LIGO - California Institute of Technology, Pasadena, CA 91125, USA

¹³LIGO - Massachusetts Institute of Technology, Cambridge, MA 02139, USA

¹⁴LIGO Hanford Observatory, Richland, WA 99352, USA

¹⁵LIGO Livingston Observatory, Livingston, LA 70754, USA

¹⁶Louisiana State University, Baton Rouge, LA 70803, USA

¹⁷Louisiana Tech University, Ruston, LA 71272, USA

¹⁸Loyola University, New Orleans, LA 70118, USA

¹⁹Max Planck Institut für Quantenoptik, D-85748, Garching, Germany

²⁰Moscow State University, Moscow, 119992, Russia

²¹NASA/Goddard Space Flight Center, Greenbelt, MD 20771, USA

²²National Astronomical Observatory of Japan, Tokyo 181-8588, Japan

²³Northwestern University, Evanston, IL 60208, USA

²⁴Salish Kootenai College, Pablo, MT 59855, USA

²⁵Southeastern Louisiana University, Hammond, LA 70402, USA

²⁶Stanford University, Stanford, CA 94305, USA

²⁷Syracuse University, Syracuse, NY 13244, USA

²⁸The Pennsylvania State University, University Park, PA 16802, USA

²⁹The University of Texas at Brownsville and Texas Southmost College, Brownsville, TX 78520, USA

³⁰Trinity University, San Antonio, TX 78212, USA

³¹Universität Hannover, D-30167 Hannover, Germany

³²Universitat de les Illes Balears, E-07122 Palma de Mallorca, Spain

³³University of Birmingham, Birmingham, B15 2TT, United Kingdom

³⁴University of Florida, Gainesville, FL 32611, USA

³⁵University of Glasgow, Glasgow, G12 8QQ, United Kingdom

³⁶University of Michigan, Ann Arbor, MI 48109, USA

³⁷University of Oregon, Eugene, OR 97403, USA

³⁸University of Rochester, Rochester, NY 14627, USA

³⁹University of Wisconsin-Milwaukee, Milwaukee, WI 53201, USA

⁴⁰Washington State University, Pullman, WA 99164, USA

⁴¹University of Manchester, Jodrell Bank Observatory, Macclesfield, Cheshire, SK11 9DL, United Kingdom
(Dated: November 18, 2018)

We place direct upper limits on the strain of the gravitational waves from 28 isolated radio pulsars by a coherent multi-detector analysis of the data collected during the second science run of the LIGO interferometric detectors. These are the first direct upper limits for 26 of the 28 pulsars. We use coordinated radio observations for the first time to build radio-guided phase templates for the expected gravitational wave signals. The unprecedented sensitivity of the detectors allow us to set strain upper limits as low as a few times 10^{-24} . These strain limits translate into limits on the equatorial ellipticities of the pulsars, which are smaller than 10^{-5} for the four closest pulsars.

PACS numbers: 04.80.Nn, 95.55.Ym, 97.60.Gb, 07.05.Kf

^aCurrently at Stanford Linear Accelerator Center

^bCurrently at Jet Propulsion Laboratory

^cPermanent Address: HP Laboratories

^dCurrently at Rutherford Appleton Laboratory

^eCurrently at University of California, Los Angeles

^fCurrently at Hofstra University

A worldwide effort is underway to detect gravitational waves (GWs) and thus test a fundamental prediction of General Relativity. In preparation for long-term operations, the LIGO and GEO experiments conducted their first science run (S1) during 17 days in 2002. The detectors and the analyses of the S1 data are described in Refs. [1] and [2]–[5], respectively. LIGO’s second science run (S2) was carried out from 14 Feb – 14 April 2003, with dramatically improved sensitivity compared to S1. During S2 the GEO detector was not operating.

A spinning neutron star is expected to emit GWs if it is not perfectly symmetric about its rotation axis. The strain amplitude h_0 of the emitted signal is proportional to the star’s deformation as measured by its ellipticity [6]. Using data from S2, this paper reports direct observational limits on the GW emission and corresponding ellipticities from the 28 most rapidly rotating isolated pulsars for which radio data is complete enough to guide the phase of our filters with sufficient precision. These are the first such limits for 26 of the pulsars. We concentrate on isolated pulsars with known phase evolutions and sky positions to ensure that our targeted search requires relatively few unknown parameters.

The limits reported here are still well above the indirect limits inferred from observed pulsar spin-down, where available (Fig. 1). However, fourteen of our pulsars are in globular clusters, where local gravitational accelerations produce Doppler effects that mask the true pulsar spin-down, sometimes even producing apparent spinup. For

these pulsars our observations therefore place the first limits that are inherently independent of cluster dynamics, albeit at levels well above what one would expect if all globular cluster pulsars are similar to field pulsars.

Our most stringent ellipticity upper limit is 4.5×10^{-6} . While still above the maximum expected from conventional models of nuclear matter, distortions of this size would be permitted within at least one exotic theory of neutron star structure [7].

Detectors. The LIGO observatory is composed of three detectors. Each detector is a power-recycled Michelson interferometer, with Fabry-Pérot cavities in the long arms. A passing GW produces a time-varying differential strain in these arms, and the resulting differential displacement of the cavity test mass mirrors is sensed interferometrically. Two detectors, the 4 km arm H1 and the 2 km arm H2 detectors, are collocated in Hanford WA. The 4 km arm L1 detector is situated in Livingston Parish LA. Improvements in noise performance between S1 and S2 were approximately an order of magnitude over a broad frequency range. Modifications that were made between S1 and S2 to aid in noise reduction and in prove stability include i) increased laser power to reduce high-frequency noise, ii) better angular control of the mirrors of the interferometer and iii) the use of lower noise digital test mass suspension controllers in all detectors.

During S2, the LIGO detectors’ noise performance in the band 40–2000 Hz was better than any previous interferometer. The best strain sensitivity, achieved by L1, was $3 \times 10^{-22} \text{ Hz}^{-1/2}$ near 200 Hz (Fig. 1). The relative timing stability between the interferometers was also significantly improved. Monitored with GPS-synchronized clocks to be better than 10 s over S2, it allowed the coherent combination of the strain data of all three detectors to form joint upper limits.

Analysis method. In [2] a search for gravitational waves from the millisecond pulsar PSR J1939+2134 using S1 data was presented. In that work, two different data analysis methods were used, one in the time domain and the other in the frequency domain. Here we extend the formal method [8] and apply it to 28 isolated pulsars.

Following [2] we model the sources as non-precessing triaxial neutron stars showing the same rotational phase evolution as is present in the radio signal and perform a complex heterodyne of the strain data from each detector at the instantaneous frequency of the expected gravitational wave signal, which is twice the observed radio rotation frequency. These data are then downsampled to $1=60 \text{ Hz}$ and will be referred to as B_k . Any gravitational signal in the data would show a residual time evolution reflecting the antenna pattern of the detector, varying over the day as the source moved through the pattern, but with a functional form that depended on several other source-observer parameters: the antenna responses to plus and cross polarisations, the amplitude of the gravitational wave h_0 , the angle between the line-of-sight to the pulsar and its spin axis, the polarisation angle of the gravitational radiation (all defined in [6]).

^gPermanent Address: GRICO, Institut d’Astrophysique de Paris (CNRS)

^hCurrently at Keck Graduate Institute

ⁱCurrently at National Science Foundation

^jCurrently at University of Sheffield

^kCurrently at Ball Aerospace Corporation

^lCurrently at European Gravitational Observatory

^mCurrently at Intel Corp.

ⁿCurrently at University of Tours, France

^oCurrently at Lightconnect Inc.

^pCurrently at W.M. Keck Observatory

^qCurrently at ESA Science and Technology Center

^rCurrently at Raytheon Corporation

^sCurrently at New Mexico Institute of Mining and Technology /

^tMagdalena Ridge Observatory Interferometer

^uCurrently at Mission Research Corporation

^vCurrently at Harvard University

^wCurrently at Lockheed-Martin Corporation

^xPermanent Address: University of Tokyo, Institute for Cosmic Ray Research

^yPermanent Address: University College Dublin

^zCurrently at Research Electro-Optics Inc.

^{aa}Currently at Institute of Advanced Physics, Baton Rouge, LA

^{bb}Currently at Thirty Meter Telescope Project at Caltech

^{cc}Currently at European Commission, DG Research, Brussels, Belgium

^{dd}Currently at University of Chicago

^{ee}Currently at LightBitt Corporation

^{ff}Permanent Address: IBM Canada Ltd.

^{gg}Currently at University of Delaware

^{hh}Permanent Address: Jet Propulsion Laboratory

ⁱⁱCurrently at Shanghai Astronomical Observatory

^{jj}Currently at Laser Zentrum Hannover

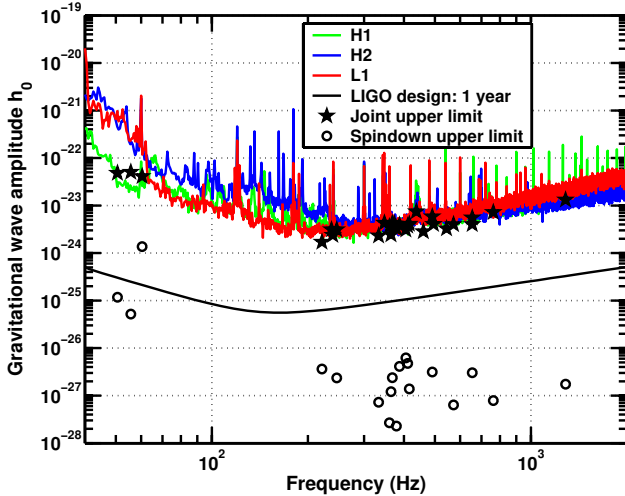


FIG. 1: Upper curves: characteristic amplitudes detectable from a known source with a 1% false alarm rate and 10% false dismissal rate, as given by Eq. (2.2) in [2], using S2 sensitivities and observation times. Lower curve: LIGO design sensitivity for 1 yr of data. Stars: upper limits found in this paper for 28 known pulsars. Circles: spindown upper limits for the pulsars with negative spin-down values if all the measured loss of angular momentum were due to gravitational waves and assuming a moment of inertia of 10^{45} g cm^2 .

and the phase ϕ_0 of the gravitational wave signal at some fiducial time t_0 . Let \mathbf{a} be a vector in parameter space with components (h_0, ψ, ϕ_0) .

The analysis proceeds by determining the posterior probability distribution function (pdf) of \mathbf{a} given the data \mathbf{B}_k and the signal model:

$$p(\mathbf{a} | \mathbf{fB}_k \mathbf{g}) / p(\mathbf{a}) p(\mathbf{fB}_k \mathbf{g} | \mathbf{a}); \quad (1)$$

where $p(\mathbf{fB}_k \mathbf{g} | \mathbf{a})$ is the likelihood and $p(\mathbf{a})$ the prior pdf we assign to the model parameters. We have used a uniform prior for $\cos \psi$, ϕ_0 , and h_0 ($h_0 > 0$), in common with [2]. A uniform prior for h_0 has been chosen for its simplicity and so that our results can readily be compared with other observations. This prior favors high values of h_0 (which comprise the majority of the parameter space) and therefore generates a somewhat conservative upper limit for its value. Indeed the reader might prefer to regard our resulting posterior pdfs for h_0 as marginalised likelihoods rather than probabilities for h_0 – these would be functionally identical using our priors.

As in [2] we use a Gaussian joint likelihood for $p(\mathbf{fB}_k \mathbf{g} | \mathbf{a})$. In [2] the S1 noise floor was estimated over a 60 s period from a 4 Hz band about the expected signal frequency. This gave a reliable point estimate for the noise level but was sensitive to spectral contamination within the band, as demonstrated in the analysis of the GEO S1 data. In this paper we exploit the improved stationarity of the instruments and take the noise floor to be constant over periods of 30 m in. In addition we restrict the bandwidth to $1=60$ Hz, which makes it possible to search for signals from pulsars at frequencies close

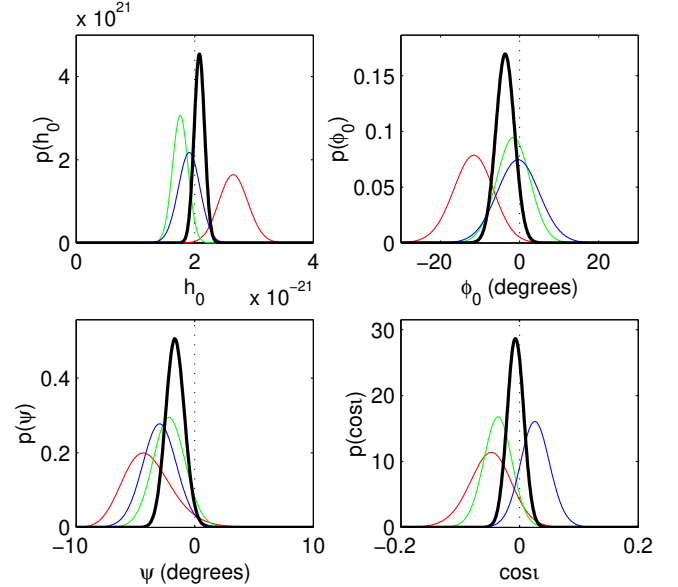


FIG. 2: Parameters of the artificial pulsar P1, recovered from 12 h of strain data from the Hanford and Livingston interferometers. The results are displayed as marginal pdfs for each of the four signal parameters. The vertical dotted lines show the values used to generate the signal, the colored lines show the results from the individual detectors (H1 green, H2 blue, L1 red), and the black lines show the joint result from combining coherently data from the three.

to strong spectral disturbances. However, the noise level now determined is less certain as the estimate relies on fewer data. We take account of this increased uncertainty by explicitly marginalising with a Jeffreys prior over the constant but unknown noise level for each 30 m in period of data [9]. The likelihood for this analysis is then the combined likelihood for all the 30 m in stretches of data, labeled by j in Eq. (2), taken as independent:

$$p(\mathbf{fB}_k \mathbf{g} | \mathbf{a}) / \prod_{j=1}^m p(\mathbf{fB}_{k_j} \mathbf{g}_j | \mathbf{a}); \quad (2)$$

$$p(\mathbf{fB}_k \mathbf{g}_j | \mathbf{a}) / \prod_{k=k_1(j)}^{k_2(j)} \mathbf{B}_k \mathbf{y}_k |^2 \mathbf{A}^j; \quad (3)$$

where \mathbf{y}_k is the signal model given by Eq. (4.10) in [2] and $m = k_2(j) - k_1(j) + 1 = 30$ is the number of \mathbf{B}_k data points in a 30 m segment.

In principle the period over which the data are assumed stationary need not be fixed, and can be adjusted dynamically to reflect instrumental performance over the run. We have limited our analysis to continuous 30 m in stretches of data, which included more than 88% of the S2 science data set. Inclusion of shorter data sections would at best have resulted in a ~6% improvement on the strain upper limits reported here (Eq. (2.2) of Ref. [2]).

Validation by hardware injections. The analysis software was validated by checking its performance on fake pulsar signals injected in artificial and real detector noise both in software ([2]) and in hardware. In particular,

two artificial signals (P1, P2) were injected into all three detectors by modulating the mirror positions via the actuation control signals with the strain signal we should expect from a hypothetical pulsar. These injections were designed to give an end-to-end validation of the search pipeline starting from as far up the observing chain as possible.

The pulsar signals were injected for a 12 h period at frequencies of 1279.123 Hz (P1) and 1288.901 Hz (P2) with frequency derivatives of zero and 10^{-8} Hz s $^{-1}$ respectively, and strain amplitudes of 2×10^{-21} . The signals were modulated and Doppler shifted to simulate sources at fixed positions on the sky with $\delta = 0$, $\cos \delta = 0$ and $\phi = 0$. To illustrate, posterior pdfs for the recovered P1 signal are shown in Fig. 2. The results derived from the different detectors are in broad statistical agreement, confirming that the relative calibrations are consistent and that the assessments of uncertainty (expressed in the posterior widths) are reasonable. Results for P2 were very similar to these.

The phase stability of the detectors in S2 allowed us to implement a joint coherent analysis based on data from all three participating instruments. This technique was noted in [2], but could not be performed on the S1 data because of timing uncertainties that existed when those observations were performed. The solid lines in Fig. 2 show marginalisations of the joint posterior from H1, H2 and L1, i.e.,

$$p(a|H1, H2, L1) / p(a)p(H1|a)p(H2|a)p(L1|a): \quad (4)$$

With three detectors of roughly similar sensitivities and operational periods these coherent results should be approximately 3 times tighter than the individual results. The posteriors for h_0 clearly highlight the relative coherence between the instruments and verify that similar joint methods can be used to set upper limits on our target pulsars.

Results. From the ATNF pulsar catalogue (www.atnf.csiro.au/research/pulsar/psrcat/) we selected 28 isolated pulsars with rotational frequencies greater than 20 Hz and for which good timing data were available (Table I). For 18 of these, we obtained updated timing solutions from regular timing observations made at the Jodrell Bank Observatory using the Lovell and the Parkes telescopes, adjusted for a reference epoch centred on the period of the S2 run (starred pulsars in Table I). Details of the techniques that were used to do this can be found in [10]. We also checked that none of these pulsars exhibited a glitch during this period.

The list includes globular cluster pulsars (including isolated pulsars in 47 Tuc and NGC 6752), the S1 target millisecond pulsar (PSR J1939+2134) and the Crab pulsar (PSR B0531+21). Although Table I only shows approximate pulsar frequencies and frequency derivatives, further phase corrections were made for pulsars with measured second derivatives of frequency. Timing solutions for the Crab were taken from the Jodrell Bank online ephemeris [11], and adjustments were made to its phase over the period of S2 using the method of [12].

pulsar	spin f (Hz)	spindown f_{-} (Hz s $^{-1}$)	$h_0^{95\%}$	
			$=10^{-24}$	$=10^{-5}$
B0021	72C	173.71	+1.50	10^{-15}
B0021	72D	186.65	+1.19	10^{-16}
B0021	72F	381.16	9.37	10^{-15}
B0021	72G	247.50	+2.58	10^{-15}
B0021	72L	230.09	+6.46	10^{-15}
B0021	72M	271.99	+2.84	10^{-15}
B0021	72N	327.44	+2.34	10^{-15}
J0030+0451		205.53	4.20	10^{-16}
B0531+21		29.81	3.74	10^{-10}
J0711	6830	182.12	4.94	10^{-16}
J1024	0719	193.72	6.95	10^{-16}
B1516+02A		180.06	1.34	10^{-15}
J1629	6902	166.65	2.78	10^{-16}
J1721	2457	285.99	4.80	10^{-16}
J1730	2304	123.11	3.06	10^{-16}
J1744	1134	245.43	5.40	10^{-16}
J1748	2446C	118.54	+8.52	10^{-15}
B1820	30A	183.82	1.14	10^{-13}
B1821	24	327.41	1.74	10^{-13}
J1910	5959B	119.65	+1.14	10^{-14}
J1910	5959C	189.49	7.90	10^{-17}
J1910	5959D	110.68	1.18	10^{-14}
J1910	5959E	218.73	+2.09	10^{-14}
J1913+1011		27.85	2.61	10^{-12}
J1939+2134		641.93	4.33	10^{-14}
B1951+32		25.30	3.74	10^{-12}
J2124	3358	202.79	8.45	10^{-16}
J2322+2057		207.97	4.20	10^{-16}

TABLE I: The 28 pulsars targeted in the S2 run, with approximate spin parameters. Pulsars for which radio timing data were taken over the S2 period are starred (*). The right-hand two columns show the 95% upper limit on h_0 , based on a coherent analysis using all the S2 data, and corresponding ellipticity values (, see text). These upper limit values do not include the uncertainties due to calibration and to pulsar timing accuracy, which are discussed in the text, nor uncertainties in r .

The analysis used 910 hours of data from H1, 691 hours from H2, and 342 hours from L1. There was no evidence of strong spectral contamination in any of the bands investigated, such as might be caused by an instrumental feature or a potentially detectable pulsar signal. A strong gravitational signal would generate a parameter pdf from inently peaked or zero with respect to its width, as for the hardware injections. Such a pdf would trigger a more detailed investigation of the pulsar in question. No such triggers occurred in the analysis of these data, and we therefore simply present upper limits.

The upper limits are presented as the value of h_0 bounding 95% of the cumulative probability of the marginalised strain pdf from $h_0 = 0$. The joint upper

lim it $h_0^{95\%}$ therefore satisfies

$$0.95 = \frac{Z_{h_0^{95\%}}}{dh_0} p(a \parallel H1, H2, L1) d d_0; \quad (5)$$

consistent with [2]. The uncertainty in the noise estimate is already included, as outlined above.

The remaining uncertainties in the upper limit values of Table I stem from the calibration of the instrument and from the accuracy of the pulsar timing models. For L1 and H2, the amplitude calibration uncertainties are conservatively estimated to be 10% and 8%, respectively. For H1, the maximum calibration uncertainty is 18%, with typical values at the 6% level. Phase calibration uncertainties are negligible in comparison: less than 10 in all detectors. Biases due to pulsar timing errors are estimated to be 3% or less for J0030+0451, and 1% or less for the remaining pulsars (see [2] for a discussion of the effect of these uncertainties).

Discussion. The improved sensitivity of the LIGO interferometers is clear from the strain upper limit for PSR J1939+2134, which is more than a factor of ten lower than was achieved with the S1 data [2]. In this analysis the lowest limit is achieved for PSR J1910-5959D at the level of 1.7×10^{-24} , largely reflecting the lower noise floor around 200 Hz.

Table I also gives approximate limits to the ellipticities [6] of these pulsars from the simple quadrupole model

$$0.237 \frac{h_0}{10^{-24}} \frac{r}{1 \text{ kpc}} \frac{1 \text{ Hz}^2}{f^2} \frac{10^{45} \text{ g cm}^2}{I_{zz}} \quad (6)$$

where r is the pulsar's distance, which we take as the dispersion measure distance using the model of Taylor and Cordes [13], and I_{zz} its principal moment of inertia about the rotation axis, which we take as 10^{45} g cm^2 .

As expected, none of these upper limits improves on those inferred from simple arguments based on the gravi-

tational luminosities achievable from the observed loss of pulsar rotational kinetic energy. However, as discussed in the introduction, for pulsars in globular clusters such arguments are complicated by cluster dynamics, which the direct limits presented here avoid.

The result for the Crab pulsar (PSR B0531+21) is within a factor of about 30 of the spindown limit and over an order of magnitude better than the previous direct upper limit of [14]. The equatorial ellipticities of the four closest pulsars (J0030+0451, J2124+3358, J1024-0719, and J1744-1134) are constrained to less than 10^{-5} .

Once the detectors operate at design sensitivity for a year, the observational upper limits will improve by more than an order of magnitude. The present analysis will also be extended to include pulsars in binary systems, significantly increasing the population of objects under inspection.

Acknowledgments. The authors gratefully acknowledge the support of the United States National Science Foundation for the construction and operation of the LIGO Laboratory and the Particle Physics and Astronomy Research Council of the United Kingdom, the Max-Planck-Society and the State of Niedersachsen/Germany for support of the construction and operation of the GEO 600 detector. The authors also gratefully acknowledge the support of the research by these agencies and by the Australian Research Council, the Natural Sciences and Engineering Research Council of Canada, the Council of Scientific and Industrial Research of India, the Department of Science and Technology of India, the Spanish Ministerio de Ciencia y Tecnología, the John Simon Guggenheim Foundation, the Leverhulme Trust, the David and Lucile Packard Foundation, the Research Corporation, and the Alfred P. Sloan Foundation. This document has been assigned LIGO Laboratory document number LIGO-P040008-A-Z.

[1] B. Abbott et al. (The LIGO Scientific Collaboration), *Nuclear Inst. and Methods in Physics Research A* 517/1-3 154 (2004).
[2] B. Abbott et al. (The LIGO Scientific Collaboration), *Phys. Rev. D* 69 082004 (2004).
[3] B. Abbott et al. (The LIGO Scientific Collaboration), *Phys. Rev. D* 69 122001 (2004).
[4] B. Abbott et al. (The LIGO Scientific Collaboration), *Phys. Rev. D* 69 102001 (2004).
[5] B. Abbott et al. (The LIGO Scientific Collaboration), *Phys. Rev. D* 69 122004 (2004).
[6] P. Jaranowski, A. Królak and B. Schutz, *Phys. Rev. D* 58 063001 (1998).
[7] B. J. Owen and D. I. Jones (2004), LIGO Technical Report T040192-00-Z,
<http://www.ligo.caltech.edu/docs/T/T040192-00.pdf>

[8] R. Dupuis and G. Wan, in preparation (2004).
[9] G. L. Bretthorst "Bayesian spectrum analysis and parameter estimation" *Lecture Notes in Statistics*, Vol 48 (Springer-Verlag, Berlin) (1988).
[10] G. Hobbs, A. G. Lyne, M. K. Kramer, C. E. Martin, and C. Jordan, *MNRAS*, in press (2004).
[11] Jodrell Bank Crab Pulsar Timing: Monthly Ephemeris, <http://www.jb.man.ac.uk/research/pulsar/crab.html>.
[12] M. Pitkin and G. Wan, *Classical and Quantum Gravity* 21 S843 (2004).
[13] J.H. Taylor and J.M. Cordes, *ApJ* 411 674 (1993).
[14] T. Suzuki, in *First Edoardo Amaldi Conference on Gravitational Wave Experiments*, edited by E. Coccia, G. Pizzella and F. Ronga (World Scientific, Singapore, 1995), p. 115.